Current Science International
Volume: 13 | Issue: 01| Jan. - March| 2024

EISSN:2706-7920 ISSN: 2077-4435
DOI: 10.36632/csi/2024.13.1.7
Journal homepage: www.curresweb.com
Pages: 87-95

Effect of Hydroxyapatite Nanoparticles Addition to Resin Modified Glass Ionomer Cement on Degree of Convergence and Fluoride Release

Nourhan I. Abdel Hafeez[1], Mohamed M. Zayed[2] and Hanaa F. Mahmoud[3]

[1]Dental Biomaterials Department, Faculty of Dentistry, Nahda University, Egypt.
[2]Operative Dentistry Department, Faculty of Dentistry, Sinai University-Kantara Branch, Egypt.
[3]Department of Biomaterials, Faculty of Dentistry, Minia University, 61519 Minia, Egypt.

Received: 25 Dec. 2023 **Accepted:** 18 Jan. 2024 **Published:** 25 Jan. 2024

ABSTRACT

Objectives: This study evaluated the effect of addition of hydroxyapatite nanoparticles to resin modified glass ionomer cement on degree of convergence and fluoride release. **Materials and Methods:** A total number of 42 specimens were prepared from Chemically cured Resin Modified Glass Ionomer (Group I) and Experimental mixture (Group II) consisting of 25% needle shaped Hydroxyapatite nanoparticles (HANPs) incorporated with Chemically cured Resin Modified Glass Ionomer, (n=21). The two tested groups were morphologically tested by SEM and chemically analyzed by EDAX after 24hrs from mixing. The degree of convergence was calculated by using transmission fourier transform infra-red spectrometer (FTIR) after 24hrs & 72hrs and fluoride release was detected at different time intervals. **Results:** The results revealed a significant decrease in the degree of convergence after 24hrs and 72hrs in Group II(A): (34.8 ±10.7 and 44.2 ± 6.8, respectively). There was a significant increase in the fluoride release for Group II(B) compared to Group I(B) among all-time intervals. **Conclusion:** addition of 25% of hydroxyapatite nanoparticles to RMGIC decreased degree of convergence and increased fluoride release property.

Keywords: Remineralization, Resin modified glass ionomer, Hydroxyapatite nanoparticles, Fluoride release Spectrophotometer, Degree of convergence, and FTIR.

1. Introduction

Different dental defects are considered as irreversible loss of dental tissues that are chemically destructed by extrinsic and intrinsic acids. The first sign of dental caries is the white spot lesions which have increased porosity and could exhibit a rough surface; however, at this stage the caries can be reversed. Current methods of preventing this problem are focused on adhesive and novel biomimetic techniques that benefit from nanotechnology. It depends on different protocols that enhance calcium phosphate remineralization, such as ions of calcium, phosphate, and mostly fluoride (Abreu *et al.,* 2023; Inchingolo *et al.,* 2023).

Remineralization is a natural repairing mechanism for recharging the hydroxyapatite crystalline structure with the lost minerals (Juntavee *et al.,* 2021). Fluoride has been recognized as a significant promoter of remineralization, and it has been used to promote fluorapatite formation, which increases the acid resistance capacity of tooth enamel (Rošin-Grget *et al.,* 2013). It prevents mineral loss from the enamel surface by stimulating surface adsorption on the partially demineralized crystals and attracting calcium and phosphate ions from oral fluid as well as producing fluorapatite on enamel surface which increases enamel resistance to acid, (Juntavee *et al.,* 2021)

One of the most used materials for tooth remineralization is glass ionomer cement (GIC) which has unique properties such as fluoride release, adhesion to tooth structure, favourable coefficient of thermal expansion, and biocompatibility. On the other hand, GIC suffers from low mechanical properties, brittleness, undesirable appearance, and moisture sensitivity at the beginning of its placement (Abreu *et al.,* 2023; Mahmoud & Metwally, 2021).

Corresponding Author: Nourhan I. Abdel Hafeez, Dental Biomaterials Department, Faculty of Dentistry, Nahda University, Egypt. E-mail: - nourhan.ibrahim@nub.edu.eg

Glass ionomer cement has many modifications to overcome those drawbacks such as Resin-modified glass ionomer cement (RMGIC). Some strategies have been applied to enhance the cross-linking and physical properties of RMGICs such as addition of hydroxyapatite (HA), metal particles, zirconia, alumina, and glass to their composition (Jalalian *et al.,* 2019).

Smart materials may function in response to specific changes occurring in the oral environment. It can neutralize acids, release therapeutic ions, suppress biofilm growth, minimize biofilm acid production, regulate the oral microbial community to prevent caries, protect enamel hardness, trigger antibacterial activity only at low pH, and treat periodontal inflammation based on enzyme response systems (Yu *et al.,* 2023).

Nanotechnology has been used to reduce any flaw size and void size, as well as stable glass particles for mechanical reinforcement (Yu *et al.,* 2023). Hydroxyapatite (HA) is similar to natural apatite found in human hard tissues. It has been used as bone grafting material, scaffolds for bone tissue engineering, dental implant coatings, soft tissue repair material, and a remineralizing agent. Hydroxyapatite nanoparticles' (HANPs) crystals have been found to promote enamel remineralization in recent research (Juntavee *et al.,* 2021).

Hydroxyapatite nanoparticles could also act as a reservoir for calcium and phosphate ions, (Juntavee *et al.,* 2021). Owing to their nano size, they can fill any small porosity on demineralized surfaces and act as a scaffold to attract calcium and phosphate from saliva to the enamel surface for the formation of a uniform new apatite layer which can completely cover the prismatic and interprismatic enamel, (Jalalian *et al.,* 2019; Juntavee *et al.,* 2021; Manchery *et al.*, 2019).

As a result, the goal of this research was to evaluate whether the addition of 25% hydroxyapatite nanoparticles to resin modified glass ionomer cement affects degree of convergence and fluoride release ability of the cement or not.

2. Materials and Methods

2.1. Experimental cement discs' preparation and grouping

Chemically cured Resin Modified Glass Ionomer (GC Fuji PLUS, GC corporation, Tokyo, Japan) supplied in powder form and polycarboxylic acid liquid was used as control group (Group I). A 25% of cement powder was replaced by Hydroxyapatite nanoparticles (HANPs) (Nanotech Egypt). In which RMGIC powder / HANPs: 3:1 ratio by weight using a digital sensitive balance (Sartorius, Entris, Goettingen, Germany) was mixed in amalgamator for 20 seconds (Rock Mix, Guangdong, China) to assure the proper powder distribution before mixing, it represented (Group II). The chemical composition of resin modified glass ionomer and Hydroxyapatite nanoparticles was shown in (Table 1).

Table 1: Composition of experimental cement used in the study.

Material	Compositions	Batch number	Manufacturer	Trade name
Resin modified glass ionomer	**Powder:** Fluoroaluminosilicate glass, initiator, pigment **Liquid:** 4-META, Phosphoric acid ester monomer, water, UDMA, dimethacrylate, silica powder, initiator, stabilizer 65%-70 %wt.	211118B	GC corporation Tokyo, Japan	(GC Fuji PLUS)
Hydroxyapatite nanoparticles	Calcium Hydroxyphosphate $Ca_{10}(PO_4)_6(OH)_2$	4028-1	Nanotech Egypt	-

A total number of 42 specimens from cement discs were prepared and divided into two groups (n=21). Group I: Conventional chemically cured RMGIC (control), and Group II: RMGIC modified by addition of HANPs (RMGIC powder / HANPs: 3/1 ratio by weight).

The cement discs for group I were prepared by mixing cement powder / liquid (2:6 ratio) on a paper pad with a spatula for 30 seconds, according to the manufacturer's instructions, whereas group II were prepared by mixing powder (RMGIC: HANPs powder)/ liquid; (6:2)/ 6 ratio. All cement groups were prepared at room temperature and controlled relative humidity.

The cement discs for each group was divided into two subgroups (n=10); in which the degree of convergence (DC) was calculated (subgroup A) and the amount of fluoride released after immersion in (deionized water) for different time intervals (subgroup B). The remaining two specimens from both groups (I&II) were used as representative specimens for morphological and chemical analysis with Scanning electron microscope (SEM) and energy dispersion x-ray analysis (EDAX).

2.2. Degree of convergence test

A total number of disc specimen's cements (n=20) (Group IA and IIA) were prepared where n=10 for each group were used in this test. Degree of convergence was measured using a Fourier Transform Infra-Red spectrometer (FTIR) (VERTEX 70, Bruker opties, Germany). The spectra were recorded in the range (400-4000 cm-1), the number of scans was 32, and the resolution was 4 cm^{-1} and scan speed 2 mm /s. The KBr transmission technique was used. Using baseline corrected original spectra, the ratio of peak intensities of aliphatic C=C to aromatic C=C (1638 / 1712 cm^{-1}, respectively) were calculated before and after curing at 24 and 72hrs from mixing to determine the percentage of remaining unreacted aliphatic C=C bonds in the mixed cements groups. Absorption of the aromatic C=C stretching band remains constant during polymerization and serves as an internal standard where the DC of each specimen was equal to 100% minus (%C=C), according to the following equation, (Jalalian *et al.,* 2019).

$$\mathrm{Dc\%} = 1 - \frac{\text{Area of C = C band } \frac{\text{Polymer}}{\text{Area}} \text{ of C = O band(polymer)}}{\text{Area of C = C band } \frac{\text{monomer}}{\text{Area}} \text{ of C = O band(monomer)}} \times 100$$

2.3. Morphology and chemical analysis for the reacted cements discs

Furthermore, after 24hrs from mixing powder and liquid according to manufacturer instruction, a selective one representative sample from each group was morphologically characterized by using SEM (Carl Zeiss Microscopy GmbH, 73447 Oberkochen, Germany). The surface elements were analyzed and identified by EDAX (Apex software using Scanning electron microscope, Weiterstadt, Germany).

2.4. Fluoride release test

A total number of disc specimens (n=20) (Group IB and IIB) were prepared. Discs were 3 mm thickness and 6 mm in diameter from each investigated group, were prepared in split Teflon molds, (Figure 1A). All cement groups were prepared as mentioned in above section (2.1.) at room temperature and controlled relative humidity, according to ISO specification #7489(Council on Dental Materials, 1989). After placement of the cement in the mold, a nylon thread was embedded into each cement disc during setting then the surface of the cement materials was covered with Mylar strips (Palermo health care, Palermo, Italy) to guard the air oxygen incorporation. All disc samples were removed from the molds after setting (20min) and polished by polishing strips (TOR VM Ltd, Moscow 119421, Russia),(Mahmoud & Metwally, 2021).

After 24hrs from mixing, each disc was individually immersed and hanged vertically by nylon thread in a polyethylene vial filled with 10 mL of deionized water, (Figure 1B). The immersed deionized water was collected, and the specimens were placed into a new clean 10 ml of deionized water. This was repeated for specific constant time interval 1, 2, 4, 7, 14, 21, 28 and 35 day. For fluoride measuring at different time intervals, Equal volumes of 2(p-Sulphophenylazo)1,8-dihydroxynaphthalene- 3,6- disulphonic acid trisodium salt (SPADNS) reagent for fluoride (Hach LANGE GmbH, Berlin, Germany) were used to buffer the collected deionized water. Then the amount of Fluoride released in deionized water was measured by using an ion digital analyser spectrophotometer (UV-VIS spectrophotometers DR 3900, Hach LANGE GmbH, Berlin, Germany) at-different time intervals; 1, 2, 4, 7, 14, 21, 28 and 35 days.

A B

Fig. 1: A: Teflon mould for Cement disc fabrication B: Samples immersed in deionized water

2.5. Statistical analysis

Statistical analysis was conducted using two-way analysis of variance (IBM SPSS Statistics for Windows, Version 23.0. Armonk, NY: IBM Corp). Mann-Whitney U test was used in comparison between the tested groups, while Wilcoxon signed-rank test was used to compare between time intervals after 24 and 72 hours within the same group (Mahmoud & Metwally, 2021).

3. Results

3.1. Results of degree of convergence (%)

The statistical analysis of different investigated groups revealed that group I(A) showed statistically significant higher percentage of degree of convergence after 24hrs than group II(A); 34.8 ±10.7 and 16.2 ±12.8%, respectively. There was a significant increase in degree of convergence after 72hrs to be (44.2 ± 6.8 and 29.8 ± 8.6%), respectively. In general, a significantly lower percentage of degree of convergence was revealed in group II(A) compared to group I(A) after 24 and 72hrs, as shown in (Table 2) and (Figure 2).

Table 2: The statistical analysis results for the comparison between degree of convergence % at different time intervals (24 and 72hrs).

Time	Group I(A) Mean ± sd	Group II(A) Mean ± sd	*P*-value
24 hours	34.8 ±10.7 Bb	16.2 ±12.8 Db	0.028*
72 hours	44.2 ± 6.8 Aa	29.8 ± 8.6 Ca	0.036*
***P*-value**	0.042*	0.043*	

M; Mean, SD; Standard deviation Means with same upper superscript letter within the same row are insignificant different Means with different superscript small letter within the same column in each group are significant different (significance < 0.005).

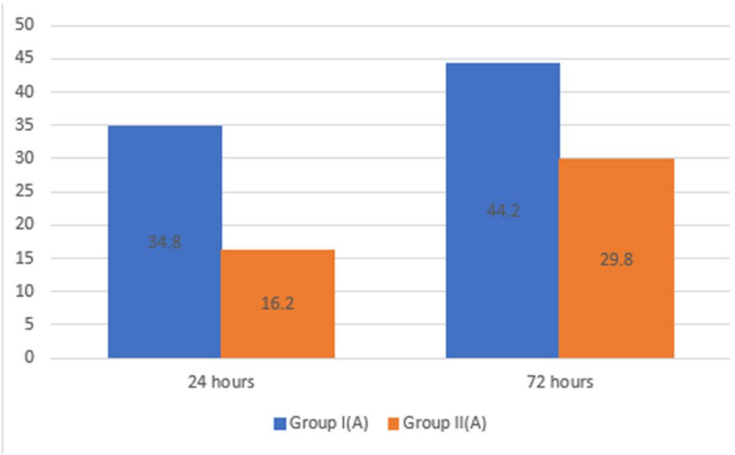

Fig. 2: Bar chart the degrees of convergence of the two groups in both time intervals

3.2. Characterization of cements after 24hrs from mixing

The SEM analysis for HANPs, RMGIC and the experimental cement was done at magnification 10.00. It was found that HANPs were needle shaped and their size ranged from 106.4 nm to 149.2 nm in length, (Figure 3(A1)). After 24hrs from mixing, group I RMGIC specimen; there were well defined opaque plates from glass particles embedded in homogeneous substrate that represent the polymeric matrix, (Figure 3(B1)), whereas group II specimen showed that aggregated clusters from the rod-like HANPs around and above the surface of the plates of the glass particles and both were imbedded in the polymeric matrix. These HANPs rods represented irregular destructed borders, and appeared like accumulated clouds in other areas, as shown in (Figure 3(C1)).

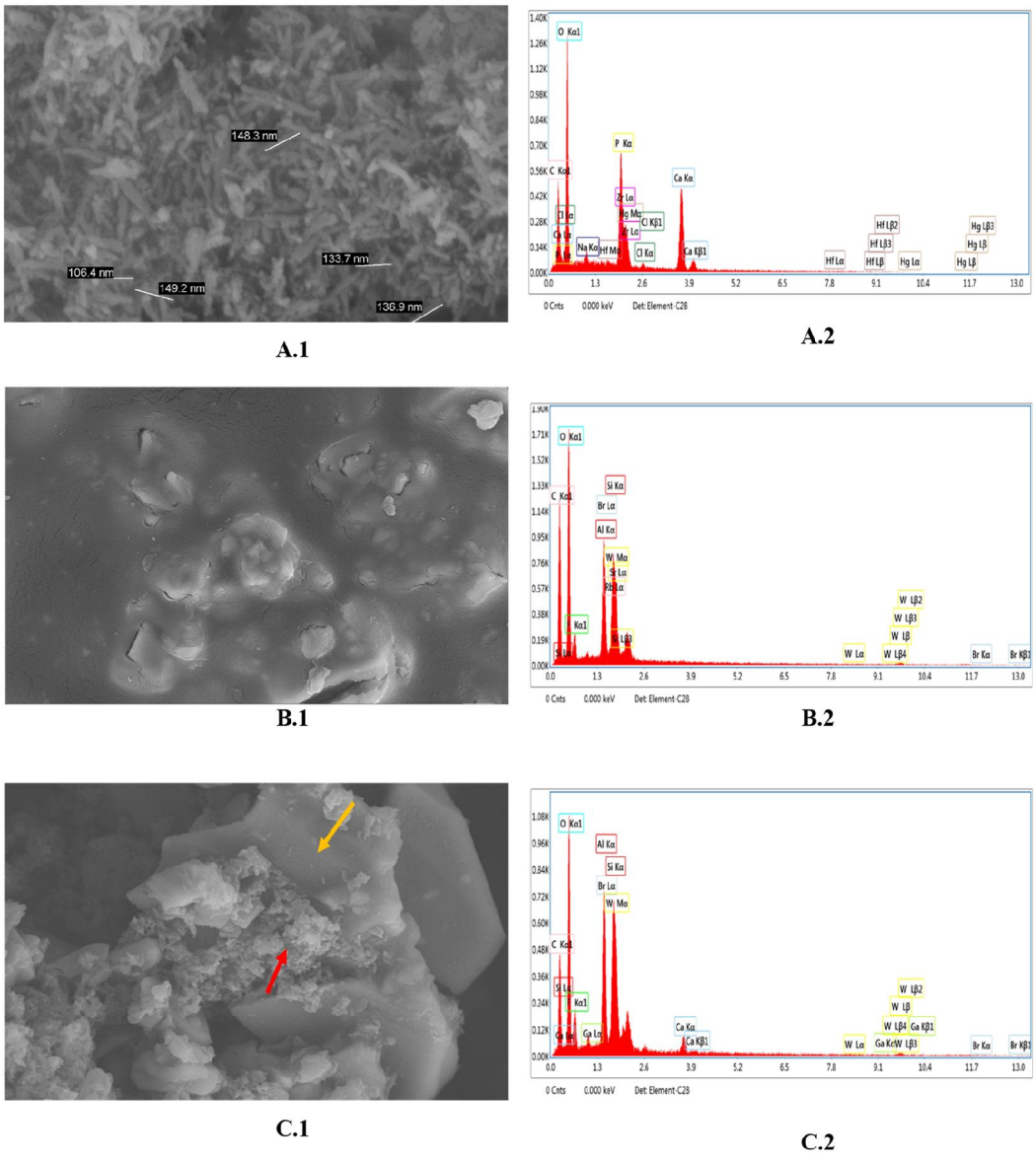

Fig. 3: A1: SEM of raw-HANPs, A2: EDAX of HANPs B1: SEM of group I after 24hrs setting, B2: EDAX group I after 24hrs setting C1: SEM group II after 24hrs setting; where (HANPs: red arrow, RMGIC: yellow arrow) and C2: EDAX of group II after 24hrs setting

The elemental analysis of the raw HANPs revealed the wt.% of Phosphorus and calcium were (10.35 and 17.29, respectively) giving 1.67 Calcium/Phosphorus ratio which is an ideal stoichiometric crystalline structure of HA. Group I contains many elements as C, O, Ca, F and Si (44.32, 48.39, 0.46, 5.34, and 1.49, respectively). On the contrary, in group II after addition of HANPs, some elements were decreased less than group I as the C, (31.63), whereas others increased as O, Ca, P, F, and Si (50.84, 3.38, 1.58, 9.1 and 3.47). Calcium/Phosphorus ratio in group II was 2.1 indicating the change of hydroxyapatite into amorphous calcium phosphate, (Table 3) and (Figure 3).

Table 3: Elemental analysis results of HANPs, and the mixed different tested cement groups after 24hrs in weight %.

Group/elements	Raw mat (NHAP) weight %	I	II
C	-	44.32	31.63
O	62.98	48.39	50.84
P	10.35	-	1.58
Ca	17.29	0.46	3.38
Ca/p	1.67		2.1
F	-	5.34	9.1
Zr	9.38	-	-
Si	-	1.49	3.47

3.3. Results of Fluoride release

The statistical analysis for the fluoride release of different groups revealed that; the maximum significant fluoride released in group I(B) was recorded after the first day (2.26±0.22 mg/l) then it decreased to the minimum significant value after day 7 to be (0.3±0.08 mg/l) and increased again after day 14 (1.71±0.29 mg/l) finally, it decreased to be steady after day 35 (0.88±0.11 mg/l). After the addition of HAPNs in group II(B); the maximum fluoride released was recorded after the first day (7.33±1.15 mg/l) which was more three times than group I(B), then it decreased to the minimum value at day 4 (0.95±0.26 mg/l) and returned to be increased again after day 14 (3.04±0.48 mg/l), finally, it decreased and remained constant till day 35 (1.73±0.16 mg/l), as shown in (Table 4) and (Figure 5 & 6). In general, group II(B) revealed a higher significant value in the amount of fluoride released along the different time intervals investigated.

Table 4: Statistical results of fluoride release (mg/l) of both groups at different time intervals

Variables	Group I	Group II	P-value
	Mean ± SD	Mean ±SD	
Day 1	2.26±0.22A	7.33±1.15A	<0.001*
Day 2	0.95±0.15B	2.51±0.63B	0.001*
Day 4	0.53±0.24C	0.95±0.26D	0.040*
Day 7	0.3±0.08D	1.09±0.37D	0.002*
Day 14	1.71±0.29B	3.04±0.48B	0.001*
Day 21	1.11±0.12C	2.45±0.29C	<0.001*
Day 28	0.79±0.16C	1.93±0.12D	<0.001*
Day 35	0.88±0.11C	1.73±0.16D	<0.001*
***P*-value**	<0.001*	<0.001*	

*: Significant at $P \leq 0.05$, Different superscripts indicate statistically significant change by time

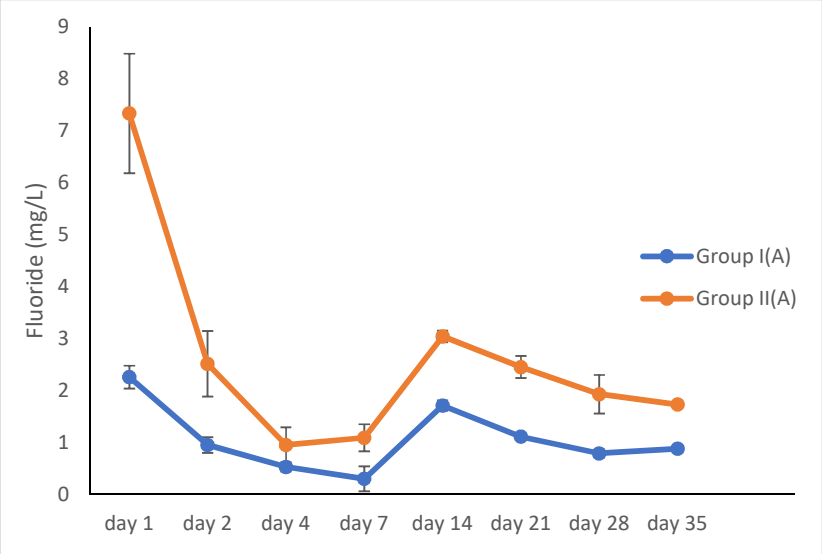

Fig. 4 : Line chart representing mean and standard deviation values for fluoride release with different interactions of variables

4. Discussion

Resin modified glass ionomer cement has favourable physical and mechanical properties, as it is easier to mix, less technique sensitive and has superior fluoride releasing property than GIC, (Sulaiman, Abdulmajeed, Altitinchi, Ahmed, & Donovan, 2019). Recently, the biomimetic concepts are processing innovative restorative material containing hydroxyapatite as one of the natural tooth constituents, (Zafar *et al.,* 2020). Hence the nano-hydroxyapatite was selected as biomimetic mineral to modify the resin modified glass ionomer. However, the biomimetic property was employed but the degree of convergence and the fluoride release ability properties were affected (Zafar *et al.,* 2020). So, in this study degree of convergence and the fluoride release were tested after adding 25% of HANPs to RMGIC.

By measuring the degree of convergence of group I(A) and group II(A) after 24hrs and after 72hrs it was found that group I(A) was statistically significantly higher in degree of convergence than group II(A) after 24hrs (34.8 ±10.7 and 16.2 ±12.8, respectively) as well as after 72hrs (44.2 ± 6.8 and 29.8 ± 8.6, respectively). This decrease in degree of convergence in group II(A) might be attributed to agglomeration of HANPs on the silica glass particles surface and in form of agglomerated cloud-like appearance this as shown in SEM, (Figure 4(C1)), (Jalalian *et al.,* 2019). The EDAX elemental analysis results revealed a decrease in carbon % on the surface after the addition of HANPs. In which, at first 24hrs in RMGIC, there were two synchronized reactions occurred: the acid base reaction and the polymerization reaction. When adding HANPs to RMGIC, there were additive competition reaction appeared due to increased calcium and phosphorus from HANPs that retard the polymerization reaction, this was assured by the decrease in the amount of carbon after addition of HANPs. The reaction started by H + ion attacking glass powder particles to be ionized to the multiple ions, then leached out to the surrounding matrix formed from poly-acrylic acid and HEMA resins. This media is acidic (PH =5) in nature in first 24hrs that led to more dissociation of HANPs crystals and transformed to amorphous non-stoichiometric hydroxyapatite crystals as shown in SEM and assured by elemental analysis as the calcium / phosphorus ratio was (2.1), and this was in agreement to Čadež *et al.* (2018); Indurkar *et al.* (2023); Vecstaudza *et al.* (2019) (Figure 4(C1)) and (Table 3). When the multi-ions consumed in the reaction and cross-linked with polymer, the degree of convergence increased after 72hrs in group I(A) and group II(A) (44.2 ± 6.8 and 29.8 ± 8.6, respectively), and this was similar to Calixto *et al.* (2013); Jalalian *et al.* (2019); Panpisut & Toneluck, 2020).

This also explains the wt.% of fluoride on the surface of the specimen in group I that was lower than that was found in group II (5.34 and 9.1), respectively, as the higher amount of resin found on the surface of group I as a result of polymerization reaction masked the fluoride found on the surface of the

specimen while in group II there was a retardation in the polymerization reaction as mentioned before so there was a less amount of resin found on the surface resulting in appearing more amount of free fluoride.

For fluoride release enhancements, the results revealed statistically significant increase (burst action) in the fluoride after the addition of HANPs (Group II(B)) initially after 24hrs (7.33±1.15) more than group I(B) (2.26±0.22) which might be attributed to the retardation of the degree of convergence as explained above. Besides, in the first 24 hrs there were multi-ions leached out and suspended in the matrix, this finding was assured from the detected fluoride amount (9.1) derived from EDAX which was higher than group I (5.34), (Table 3). With the increased degree of convergence of both groups, the fluoride releasing intensities decreased, this might be attributed to increase in the cross-linked multi-ions so fluoride entrapped, which was according to Kumari *et al.* (2019); Mahmoud & Metwally, (2021). It was found that, the fluoride declined in release after day 4 in the group II(B) (0.95±0.26) while after 7 days in group I(B) (0.3±0.08). The amount of degree of convergence after the HANPs addition (Group II(A)) was higher than group I(A) at 72hrs (13.6 and 9.4, respectively), this explained the fast decrease in fluoride releasing at day 4 in group II(B) while at day 7 for group I(B).

The fluoride releasing returned to increase in day 14 in group I(B) and group II(B) (3.04±0.48 and 1.71±0.29, respectively) which might be explained as in this study flow technique was used in immersion of the specimens and this led to destruction of the surface and leaching out of more ions. Finally, fluoride release decreased and remained constant till day 35 which be might attributed disintegration of the total amount of fluoride ions inside the specimen, and these results were in agreement to Abdallah & Ibrahim, (2019); Mahmoud & Metwally, (2021).

Generally, similar to Mahmoud & Metwally, (2021); Murugan *et al.* (2022), the results revealed a statically significant increase in fluoride release in group II(B) after addition of HANPs in all time intervals which might be explained by the larger surface area of HANPs that led to the increased acid-base reaction an delayed polymerization which was explained by degree of convergence results,

As a result, the addition of 25% hydroxyapatite nanoparticles decreased the degree of convergence and increased fluoride release ability of the cement.

5. Conclusion

Under the limitations of this study

Addition of 25% of HANPs to RMGIC decreased the degree of convergence and increased fluoride releasing property which enhances the remineralization effect and anti-cariogenic potential of RMGIC.

References

Abdallah, A.M., T.M. Elshehawy, and H.M. Ibrahim, 2019. Fluoride Release and Recharge Behavior of Bioactive Glass Ionomer Cements using Ion Chromatography. Egyptian Dental Journal, 65(1), 399-406. doi:10.21608/edj.2019.72715.

Abreu, J.D., S.D.O. Silva, A.A. Amorim, E. José Soares, R. Geng-Vivanco, C.N.F.D. Arruda, and F.D.C.P. Pires-de-Souza, 2023. Incorporation of bioactive glass-ceramic into coconut oil for remineralization of incipient carious lesions. Brazilian Dental Journal, 34(6): 82-90. doi:10.1590/0103-6440202305636

Čadež, V., I. Erceg, A. Selmani, D. Domazet Jurašin, S. Šegota, D.M. Lyons, and M.D. Sikirić, 2018. Amorphous Calcium Phosphate Formation and Aggregation Process Revealed by Light Scattering Techniques. Crystals, 8(6): 254. doi:10.3390/cryst8060254

Calixto, L.R., M.R. Tonetto, S.C. Pinto, E.D. Barros, A.H. Borges, F.V. Lima, and M.C. Bandéca, 2013. Degree of conversion and hardness of two different systems of the Vitrebond™ glass ionomer cement light cured with blue LED. J Contemp Dent Pract., 14(2): 244-249. doi:10.5005/jp-journals-10024-1307

Council on Dental Materials, I., and Equipment. 1989. ANSI/ADA specification no. 66 for dental glass ionomer cements. J Am Dent Assoc., 119(1): 205.

Inchingolo, F., G. Dipalma, D. Azzollini, I. Trilli, V. Carpentiere, D. Hazballa, and A. Inchingolo, M. 2023. Advances in Preventive and Therapeutic Approaches for Dental Erosion: A Systematic Review. Dentistry Journal (Basel), 11(12), 274. doi:10.3390/dj11120274

Indurkar, A., R. Choudhary, K. Rubenis, M. Nimbalkar, A. Sarakovskis, A.R. Boccaccini, and J. Locs, 2023. Amorphous Calcium Phosphate and Amorphous Calcium Phosphate Carboxylate: Synthesis and Characterization. ACS Omega, 8(30): 26782-26792. doi:10.1021/acsomega.3c00796

Jalalian, B., P. Golkar, A. Paktinat, E. Ahmadi, S.A. Panahande, and L.R. Omrani, 2019. Degree of Conversion of Resin-Modified Glass Ionomer Cement Containing Hydroxyapatite Nanoparticles. Front Dent, 16(6): 415-420. doi:10.18502/fid.v16i6.3440

Juntavee, A., N. Juntavee, and P. Hirunmoon, 2021. Remineralization Potential of Nanohydroxyapatite Toothpaste Compared with Tricalcium Phosphate and Fluoride Toothpaste on Artificial Carious Lesions. Int J Dent., 5588832. doi:10.1155/2021/5588832

Kumari, P.D., S. Khijmatgar, A. Chowdhury, E. Lynch, and C.R. Chowdhury, 2019. Factors influencing fluoride release in atraumatic restorative treatment (ART) materials: A review. J Oral Biol Craniofac Res, 9(4): 315-320. doi:10.1016/j.jobcr.2019.06.015

Mahmoud, N., and A. Metwally, 2021. Fluoride Release and Recharging Ability of Glass Ionomer Cement Incorporating Hydroxyapatite Nanoparticles. Egyptian Dental Journal, 67(4): 3741-3749. doi:10.21608/edj.2021.89027.1732

Manchery, N., J. John, N. Nagappan, G.K. Subbiah, and P. Premnath, 2019. Remineralization potential of dentifrice containing nanohydroxyapatite on artificial carious lesions of enamel: A comparative in vitro study. Dent Res J (Isfahan), 16(5): 310-317.

Murugan, R., F. Yazid, N.S. Nasruddin, and N.N.M. Anuar, 2022. Effects of Nanohydroxyapatite Incorporation into Glass Ionomer Cement (GIC). Minerals, 12(1): 9.

Panpisut, P., and A. Toneluck, 2020. Monomer conversion, dimensional stability, biaxial flexural strength, and fluoride release of resin-based restorative material containing alkaline fillers. Dent Mater J, 39(4): 608-615. doi:10.4012/dmj.2019-020

Rošin-Grget, K., K. Peroš, I. Sutej, and K. Bašić, 2013. The cariostatic mechanisms of fluoride. Acta Med Acad., 42(2): 179-188. doi:10.5644/ama2006-124.85

Sulaiman, T.A., A.A. Abdulmajeed, A. Altitinchi, S.N. Ahmed, and T.E. Donovan, 2019. Physical Properties, Film Thickness, and Bond Strengths of Resin-Modified Glass Ionomer Cements According to Their Delivery Method. J Prosthodont, 28(1): 85-90. doi:10.1111/jopr.12779

Vecstaudza, J., M. Gasik, and J. Locs, 2019. Amorphous calcium phosphate materials: Formation, structure and thermal behaviour. Journal of the European Ceramic Society, 39(4): 1642-1649. doi:10.1016/j.jeurceramsoc.2018.11.003

Yu, K., Q. Zhang, Z. Dai, M. Zhu, L. Xiao, Z. Zhao, and K. Zhang, 2023. Smart Dental Materials Intelligently Responding to Oral pH to Combat Caries: A Literature Review. Polymers (Basel), 15(12). doi:10.3390/polym15122611

Zafar, M.S., F. Amin, M.A. Fareed, H. Ghabbani, S. Riaz, Z. Khurshid, and N. Kumar, 2020. Biomimetic Aspects of Restorative Dentistry Biomaterials. Biomimetics (Basel), 5(3). doi:10.3390/biomimetics5030034